DETERMINATION OF INITIAL Sr ISOTOPIC COMPOSITIONS OF DOLOSTONES FROM THE BURLINGTON-KEOKUK FORMATION (MISSISSIPPIAN): CONSTRAINTS FROM CATHODOLUMINESCENCE, GLAUCONITE PARAGENESIS AND ANALYTICAL METHODS[1]

JAY L. BANNER,[2] G. N. HANSON, AND W. J. MEYERS
Department of Earth and Space Sciences
State University of New York
Stony Brook, New York 11794

ABSTRACT: Regionally extensive, fine-grained dolostones from the Mississippian Burlington-Keokuk Fm. comprise two major generations of dolomite that can be distinguished by their cathodoluminescence, chemical compositions, and times of formation. The petrography and geochemistry of glauconite, the predominant clay mineral in the dolostones, indicates that it is an authigenic phase, some of which formed episodically during various stages of postmarine diagenesis. This study evaluates techniques for the determination of the Sr isotopic compositions of the dolomite generations through the analysis of nearly pure whole-rock samples (≥ 95% soluble) and mineral separates, each composed predominantly of one cathodoluminescent type of dolomite.

Sr isotopic compositions and Rb and Sr concentrations were measured on samples prepared by three separate methods: 1) leaching with 1.25N HCl, 2) leaching with 1.25N HCl and concentrated HF, and 3) complete dissolution with concentrated HF and HNO_3, and 6N HCl. Leaching with HCl removes 24–60 percent of the Rb in the samples. Compared to acid leaching, complete sample dissolution yields higher $^{87}Sr/^{86}Sr$ ratios and Rb concentrations and more reproducible results. This indicates that most of the Rb and radiogenic ^{87}Sr is associated with minor clay fractions in the samples and that HCl leaches Rb and Sr from clays to a variable extent.

The relatively high Rb/Sr ratios of the dolostones necessitate an age correction of each sample's $^{87}Sr/^{86}Sr$ ratio. The determination of such initial $^{87}Sr/^{86}Sr$ ratios requires contemporaneous formation of carbonate and clay, closure of the Rb-Sr system after diagenesis, and constraints on the timing of diagenesis. Calculated initial $^{87}Sr/^{86}Sr$ ratios for the dolostones by method 3 differ considerably from the uncorrected measured $^{87}Sr/^{86}Sr$ ratios by any of the dissolution methods. These results demonstrate that even minor clay components can make significant contributions to the analyses, and that analysis for Rb and Sr, and constraints on the timing and diagenetic history of both the clay and carbonate phases can be critical for the determination of the Sr isotopic compositions of even nearly pure dolostones. An evaluation of the uncertainties associated with the timing and type of diagenesis indicates that the initial $^{87}Sr/^{86}Sr$ ratios of the dolostones are representative of the isotopic composition of the dolomite generations at the time of their formation.

Two major cathodoluminescent types of Burlington-Keokuk dolomites preserve a record of two isotopically distinct diagenetic environments. Samples composed of the earliest dolomite (dolomite I) have initial $^{87}Sr/^{86}Sr$ ratios ranging from 0.70757 to 0.70808, while samples composed of dolomites II and II′ range from 0.70885 to 0.70942.

INTRODUCTION

The isotopic composition of strontium in carbonate rocks has become an important diagnostic tool for diagenetic and paleoceanographic studies. The application of Sr isotopes to understanding carbonate diagenesis has been fostered by 1) the analysis of natural fluids such as modern seawater, river water, and subsurface brines for Sr isotopes (Chaudhuri 1978; Sunwall and Pushkar 1979; Stueber et al. 1984; McNutt et al. 1984; Wadleigh et al. 1985; Chaudhuri et al. 1987; Goldstein and Jacobsen 1987), and 2) the construction and refinement of a "seawater curve" of $^{87}Sr/^{86}Sr$ through time, based on analyses of marine carbonates of known age (Peterman et al. 1970; Veizer et al. 1983; Burke et al. 1982; DePaolo and Ingram 1985; Palmer and Elderfield 1985; Kaufman et al. 1986; Koepnick et al. 1985a; DePaolo 1986; Hess et al. 1986; Popp et al. 1986). Diagenetic carbonates can have Sr isotopic compositions that deviate from the marine value, and these variations can be ascribed to either various nonmarine diagenetic processes, or to diagenesis by younger seawater of different isotopic composition. These approaches have been particularly useful towards addressing some fundamental questions regarding dolomitization (Saller 1984; Stueber et al. 1984; Koepnick et al. 1985b; Aharon et al. 1987; Swart et al. 1987).

The dolomites of the Mississippian Burlington and Keokuk Fms. are massively bedded and regionally extensive. The two formations have had similar depositional and diagenetic histories, and formational boundaries are not distinguished in many parts of the study area. Therefore, they will be referred to hereafter as the Burlington-Keokuk Fm. Cathodoluminescent petrography defines at least five different episodes of dolomitization and can be used to select nearly pure whole-rock samples (dolostones) that represent a single diagenetic phase. The utility of Sr isotopes in constructing quantitative models for water-rock interaction, including dolomitization in the Burlington-Keokuk Fm., is discussed in Banner (1986) and Banner et al. (1988a).

The purpose of the present study is to develop an approach to determine the Sr isotopic compositions of the dolomites of the Burlington-Keokuk Fm. at the time of their crystallization. The accurate determination of the dolomite Sr isotopic compositions from the analysis of whole-rock and mineral separate samples requires careful analytical and petrologic considerations.

Leaching of whole-rock carbonate samples with weak HCl is a standard dissolution method for obtaining carbonate-selective geochemical analyses of impure samples. It has been recognized, however, that Na, Fe, Mn, and rare earth elements in various noncarbonate phases can

[1] Manuscript received 28 August 1986; revised 6 January 1988.

[2] Present address: Division of Geological and Planetary Sciences, California Institute of Technology, Pasadena, CA 91125 (corresponding), and Basin Research Institute, Louisiana State University, Baton Rouge, LA 70803.

JOURNAL OF SEDIMENTARY PETROLOGY, VOL. 58, NO. 4, JULY, 1988, P. 673–687
 0022-4472/88/0058-0673/$03.00

be quantitatively leached by weak acid (Veizer 1983; Banner et al. 1988b). The effects of leaching can be severe in the case of $^{87}Sr/^{86}Sr$ analyses of carbonates because the noncarbonate phases may have relatively large concentrations of Rb, which decays to produce radiogenic ^{87}Sr ($^{87}Rb \rightarrow {}^{87}Sr + \beta^-$). In particular, clays such as glauconite and illite can have high Rb and radiogenic ^{87}Sr contents residing in the interlayer cation sites in the phyllosilicate structure. Glauconite is the only microscopically observed clay mineral in the dolostones although small percentages of other, fine-grained clay mineral phases may be present. The term *clay*, when used in reference to the Burlington-Keokuk dolostones, will refer to all clay mineral phases in a sample.

Rb-Sr geochronologic studies of glauconite, illite, and other clay minerals indicate that 1) gentle leaching agents such as 0.5N HCl, NH_4-EDTA, ammonium acetate, dodecyl- and hexadecyl-ammonium chloride, and silver thiourea extract Rb and Sr from some phyllosilicates (Thompson and Hower 1973; Kralik 1984; Long and Agee 1985; Morton 1985), and 2) acid leaching may remove Rb and Sr from different sites in glauconite (Thompson and Hower 1973). Therefore, for Rb-Sr analyses of dolostones with significant amounts of clay, leaching with acid of sufficient strength to dissolve dolomite may be neither carbonate-selective nor clay-site-selective.

Of primary interest to studies of carbonate diagenesis is the Sr isotopic composition of a diagenetic phase at the time of its formation (initial $^{87}Sr/^{86}Sr$ ratio), which can provide important information about the fluid from which it was derived. For such a determination, it is necessary to correct the measured Sr isotopic composition of a phase using its age and Rb/Sr ratio. Radiogenic ^{87}Sr contents are negligible in young carbonates and clays, or in carbonates with very low Rb/Sr ratios (e.g., DePaolo and Ingram 1985; Kaufman et al. 1986). However, $^{87}Sr/^{86}Sr$ analyses of the Burlington-Keokuk dolostones require significant age corrections, owing to the relatively high Rb and low Sr concentrations of these samples.

Comparative dissolution experiments were conducted on Burlington-Keokuk dolostones and mineral separates, both consisting predominantly of a single type of cathodoluminescent dolomite, in order to evaluate 1) the utility of acid leaching for whole-rock analyses of $^{87}Sr/^{86}Sr$ ratios and Rb and Sr abundances, and 2) the contributions of noncarbonate phases to whole-rock analyses. The results of experiments using leaching and complete dissolution show that minor amounts of noncarbonate contaminants in nearly pure Burlington-Keokuk dolostones make significant contributions to whole-rock analyses, and it is thus essential to correct the analyses for such contaminants. Dolostone whole-rock Sr isotope analyses will be particularly sensitive to even 2–3 percent of clay minerals with high Rb contents typical of glauconite.

Deciphering the diagenetic history of both the carbonate and the clay portions of the Burlington-Keokuk dolostones is critical for the determination of the Sr isotopic composition of the dolomites at the time of dolomitization: 1) If the clay and carbonate minerals in a whole-rock carbonate sample formed contemporaneously from the same fluid (during deposition or diagenesis), then each mineral and the whole-rock will have the same initial $^{87}Sr/^{86}Sr$ ratio. 2) If the clay is detrital and derived from older crust, it will have a significantly higher $^{87}Sr/^{86}Sr$ ratio than the carbonate throughout the whole-rock sample's history, and an initial $^{87}Sr/^{86}Sr$ ratio determined on such a whole-rock sample will be unrepresentative of either phase's initial isotopic composition. In this context, an examination of the petrography and geochemistry of glauconite in the dolostones points to an authigenic origin for the glauconite, some of which formed during several episodes of postmarine diagenesis.

For carbonate samples with significant detrital components, it may be necessary to develop reproducible and selective leaching methods, or to determine end-member components of a sample's $^{87}Sr/^{86}Sr$ inventory by sequential leaching (e.g., DePaolo et al. 1983; Kralik 1984). Using limits provided by the paragenesis and geochemistry of glauconite and the cathodoluminescent stratigraphy of dolomite and calcite, the Sr isotopic composition of the different dolomite generations in the Burlington-Keokuk Fm. will be determined by calculating initial $^{87}Sr/^{86}Sr$ ratios from analyses of Rb and Sr abundances and $^{87}Sr/^{86}Sr$ ratios on completely dissolved, nearly pure dolostones and dolomite separates.

PETROGRAPHY

The Burlington-Keokuk Fm. crops out in Iowa, Illinois, and Missouri as part of the Osage Series of the Mississippian system (Fig. 1). These strata comprise medium- to thick-bedded crinoidal grainstones and packstones interbedded with pervasively dolomitized lime mud in mudstones and wackestones. Chert nodules and lenses are abundant, and thin, shaly units and glauconite- and phosphate-rich horizons are common.

Cathodoluminescence is used to 1) distinguish different generations of dolomite and establish their relative times of formation on a regional scale; 2) time the formation of the dolomites relative to the calcite cement zones, which in turn have been timed absolutely by stratigraphic constraints (Harris 1982; Kaufman et al. 1988); and 3) establish timing relationships between glauconite and diagenetic carbonates.

Dolostones

Massive dolomites (dolostones) consist of 25–150-micron rhombs with variable proportions of other phases. These include pelletoidal glauconite and finely dispersed clays, disseminated pyrite, marcasite and pyrrhotite, iron oxide coatings on rhombs, phosphatic fin spines and teeth, replacive chert and quartz cements and siliceous sponge spicules, two major generations of calcite cements (early nonferroan and late ferroan), and calcitic fossils (crinoids, bryozoans, brachiopods, and corals). One- and two-phase fluid inclusions and mineral inclusions occur in varying abundances in the dolomite rhombs. The most common accessory phases in the dolostones are pyrite, calcite, glauconite, and chert.

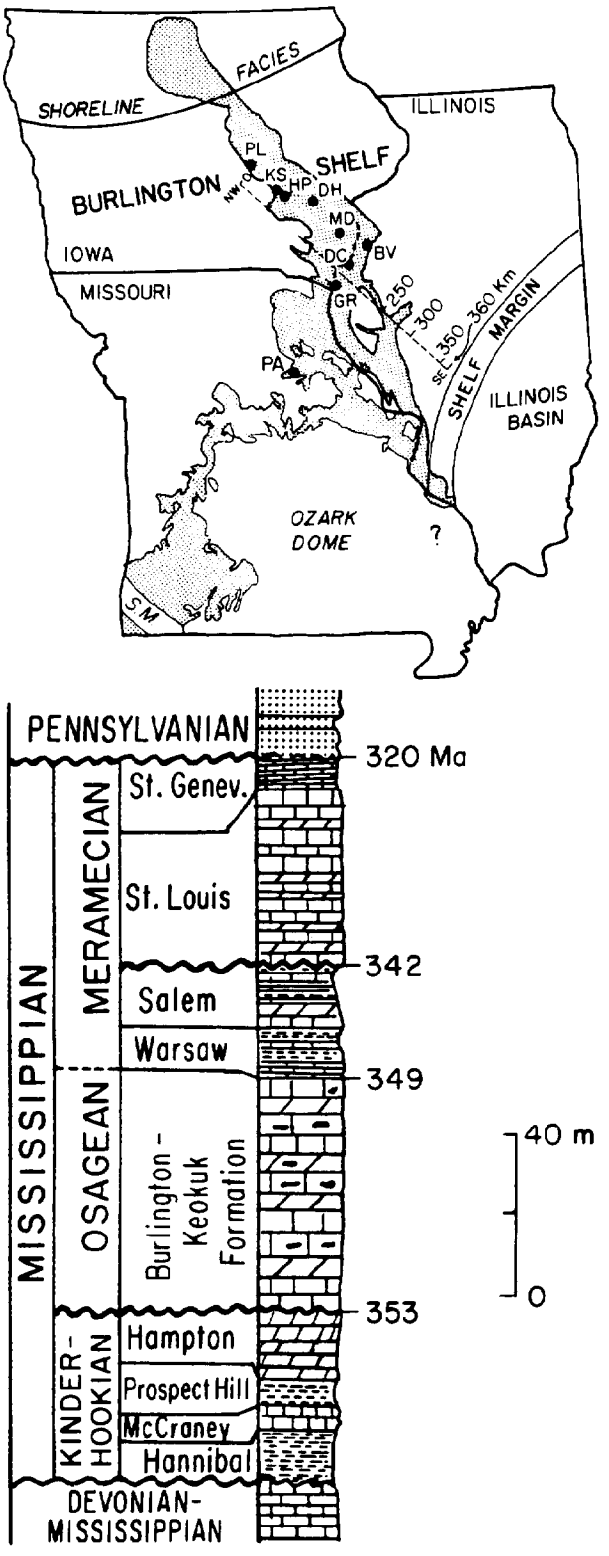

FIG. 1.—Paleogeographic sketch map showing sample localities in Iowa, Illinois, and Missouri. Stippled area shows outcrop pattern of Mississippian rocks. Paleogeography after Lane and DeKeyser (1980); inferred shoreline facies from Sixt (1984). Generalized stratigraphic section of Mississippian rocks in western Illinois after Harris (1982). ← Stratigraphic time scale from Harland et al. (1982). Samples from the following quarries were analyzed: BV = Biggsville; DH = Don Hays; DC = Dallas City; GR = Gray's; HP = Harper; KS = Keswick; MD = Mediapolis; PA = Paris; PL = Puls-Malcolm.

Cathodoluminescent petrography defines two major and at least three minor generations of dolomite. Dolomite I, the earliest dolomite, forms concentrically zoned yellow to orange to light brown luminescent rhombs (Fig. 2b). Dolomite II replaced dolomite I and has a dull red, unzoned luminescence (Fig. 2c). The truncation of the fine-scale growth banding in dolomite I by dull red patches of dolomite II demonstrate the replacement relationship (Fig. 3c). The similar sizes of dolomite I and II rhombs within a single sample are consistent with this timing sequence. Dolomite II′ is a volumetrically minor dolomite with chocolate brown cathodoluminescence that replaces both older dolomites. Dolomites II and II′ have similar textural appearances and both are more stoichiometric and iron-rich compared to dolomite I (Prosky and Meyers 1985; Prosky et al. 1986). Dolomite III is a nonluminescent cement and replacement (Harris 1982) which postdates dolomites I, II, and II′, and its minor occurrence as a syntaxial overgrowth on older rhombs prevented isotopic analysis of this dolomite. Iron concentrations increase through the sequence dolomite I-II-II′-III (Prosky and Meyers 1985). Saddle dolomite is also nonluminescent and fills solution vugs which postdate all other dolomites in the field area.

Timing of Diagenesis

The cathodoluminescent zonal stratigraphy of calcite cements and dolomite rhombs and cements in the Burlington-Keokuk Fm. allows the relative times of formation of various diagenetic phases to be determined. Similar timing relationships also constrain two major generations of postmarine calcite cementation in the Burlington-Keokuk Fm. to have occurred during Mississippian and Pennsylvanian–Early Permian time (Harris 1982; Kaufman et al. 1988). Deflection geometries and truncation of first-generation calcite cement zones around dolomite rhombs, and calcite cements infilling partially dissolved rhombs are observed in packstones and grainstones under cathodoluminescence. These features constrain the formation of dolomite I to have preceded nearly all calcite cementation, and they are consistently observed on a regional scale (Harris 1982; Kaufman et al. 1988).

The comparison of calcite zonal stratigrapies in the overlying St. Louis Fm. and younger units with the Burlington-Keokuk cement sequence suggest that first-generation cementation occurred at the earliest during a pre-St. Louis unconformity (Fig. 1). First-generation calcite cements are engulfed by Pennsylvanian clastic sediments within pre-Pennsylvanian karst cavities in central Missouri, indicating that first-generation cements formed at the latest time prior to Pennsylvanian time (Kaufman et al. 1988). The pattern of cathodoluminescent zonation in dolomite I rhombs is similar within many measured sections but differs between localities (Cander et al. 1988;

Prosky, unpubl. data), constraining the formation of dolomite I to postdate deposition of the Burlington-Keokuk Fm. These observations indicate an age range for dolomite I formation from post-Osagean to pre-Pennsylvanian.

First-generation calcite cement zones show the same deflection geometries around dolomite II and II′ rhombs, but owing to the replacement texture of dolomites II and II′, geometrical timing relationships with calcite cement zones are not as obvious compared to dolomite I–calcite cement timing relationships. Dolomite II predates some nodular chertification of pre-Pennsylvanian age (Cander et al. 1988). The most straightforward inference from these observations is a postdolomite I, pre-Pennsylvanian age for dolomites II and II′. A pre–Early Permian upper age limit for dolomite II is based on a pre-second generation calcite cement timing for dolomite II (Kaufman et al. 1988). For the purposes of calculating initial $^{87}Sr/^{86}Sr$ ratios, an age of 342 Ma for dolomites I, II, and II′ was used in Table 2, and the effect of the age uncertainty on these values is illustrated in the Discussion section.

Glauconite

The predominant clay mineral in the Burlington-Keokuk Fm. is glauconite. It is particularly abundant in mudstone to wackestone textures, commonly occurring as deep-green pellets, approximately 500 microns across in longest dimension, with a microcrystalline internal texture. Less commonly, glauconite is anhedral and finely dispersed. All forms of glauconite observed in Burlington-Keokuk rocks are nonluminescent at electron beam conditions of 10–12 kV and 0.6–0.8 mA. Most of the dispersed (< 5 μm) glauconite was identified using its distinctive relief, color, birefringence, and nonluminescence, while in some cases it was identified by electron microprobe analysis.

The nonpelletoidal glauconite occurs 1) as inclusions in dolomite rhombs and in calcite cements, 2) as partial skeletal replacements and pore fillings in fossils, 3) as partial to complete fillings of fractures and interrhomb porosity, and 4) along stylolite seams. These occurrences are most common in samples which have greater than five modal percent glauconite pellets. In instances where it is clear that the dispersed glauconite is authigenic rather than remnants of disaggregated crystals, the timing of the formation of the dispersed glauconite relative to other diagenetic phases may be established.

Rhombs can have cores containing finely crystalline glauconite, and in some instances concentric cathodoluminescent zones in the dolomite parallel the form of the glauconite in the core. This is indicative of either glauconite dissolution and dolomite overgrowth on the remaining nucleus, or dolomite replacement of glauconite. In either case, dolomitization postdates glauconite formation. Glauconite inclusions in some dolostones are aligned parallel to the rhomb faces (Fig. 3a), indicating that the glauconite formed during the growth of the dolomite. In these instances, the portion of the dolomite rhomb in which the inclusions are concentrated has a

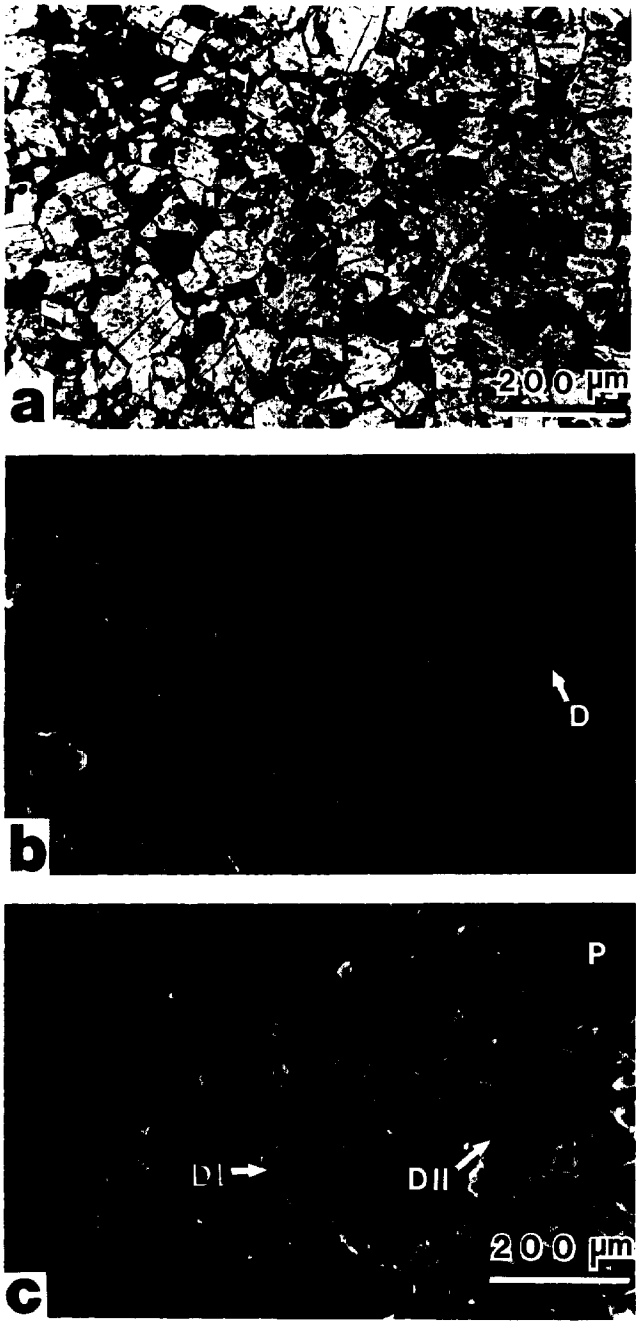

FIG. 2.—Major cathodoluminescent types of dolomite in the Burlington-Keokuk Fm. a) Dolomite I sample in plane-polarized light. Euhedral to subhedral rhombs. Some larger rhombs have inclusion-rich cores. Finely crystalline iron oxides (goethite) coat many rhombs. Dark circles are bubbles in epoxy. Sample DH-8. b) Same field of view as in (a) under cathodoluminescence. Concentric zonation, fine-scale light and dark growth bands and yellow to light brown luminescence characterize dolomite I. Dissolution of dolomite shown at D. c) Dolomite II sample under cathodoluminescence. Dull red luminescence (DII) illustrates preferential replacement of the interiors of precursor dolomite I rhombs, leaving bright yellow rims. Different stages of recrystallization can be observed from unscathed dolomite I rhomb (DI) to pervasive replacement. P = porosity. Sample KS-6.

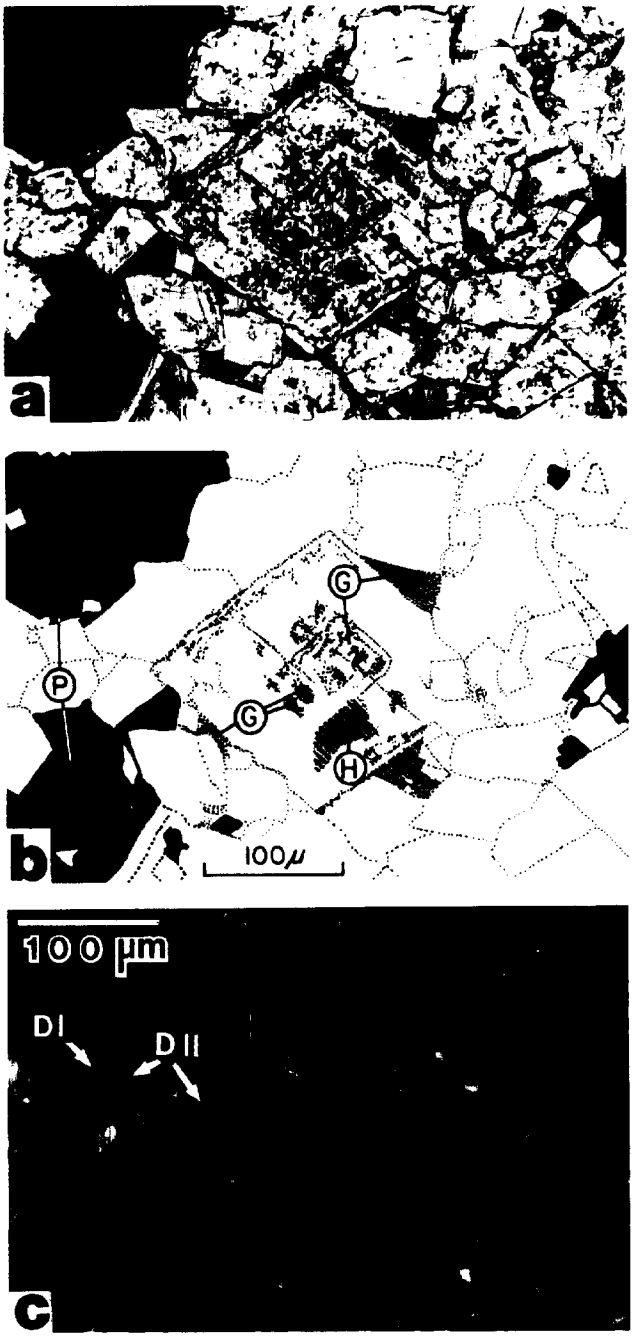

FIG. 3.—Dolomite II rhomb containing inclusions of glauconite. a) Photomicrograph in plane-polarized light and sketch in (b). Glauconite occurs as green inclusions in rhombs (G) and partial to complete anhedral fillings of rhomb interstices (G), and most commonly as ellipsoidal pellets (not shown). Note general alignment of glauconite inclusions parallel to growth faces of rhomb, suggesting contemporaneous formation of glauconite and dolomite. Interstitial glauconite postdates dolomite formation. P = porosity, H = hole. c) Same field of view under cathodoluminescence. Dull red dolomite II (DII) with bright rims of dolomite I showing zonation (DI). Sharp truncation of dolomite I growth banding against dolomite II illustrates relative ages of the dolomites as discussed in the text. Note dark core of large rhomb where both glauconite and dolomite occur. Darker luminescence in Burlington-Keokuk dolomites reflect higher iron content (Prosky et al. 1986). This is indicative of the contemporaneous formation of relatively iron-rich dolomite and glauconite. Sample HP-4-GR.

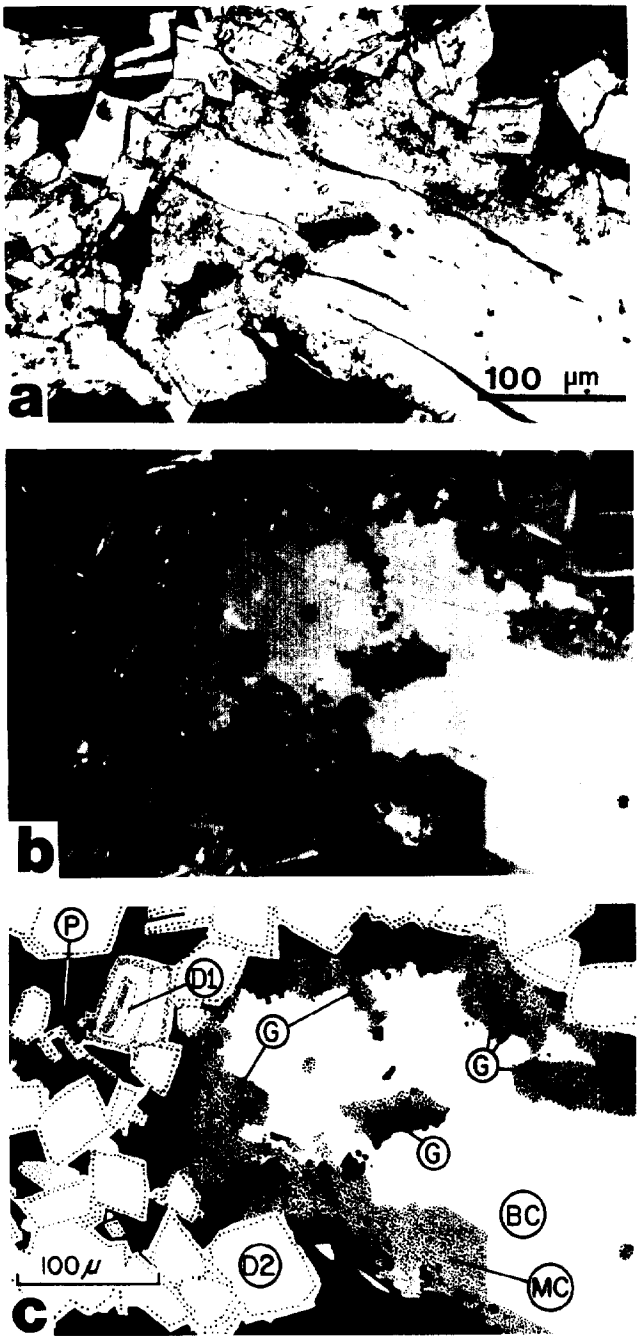

FIG. 4.—Dolomite-calcite cement-glauconite timing relationships. a) plane-polarized light, b) cathodoluminescence, c) labeled sketch of cathodoluminescence photo. D1 = dolomite I; D2 = dolomite II; BC = calcite cement zone with bright luminescence; MC = calcite cement zone with moderate luminescence; G = nonluminescent glauconite inclusions in calcite cement. Calcite cement crystallized after the formation of dolomite, as indicated by the infilling of porosity created by dolomite rhombs, most noticeably in upper right quadrant of (b). Larger glauconite inclusions in bright calcite cement may have formed prior to cementation and subsequently became engulfed. The smaller inclusions in the moderate calcite (MC) were more likely formed during the growth of this later cement. Similar to the glauconite-dolomite relationships illustrated in Figure 3, glauconite appears to have formed contemporaneously with relatively iron-rich calcite cement. Luminescent character of calcite cement is similar to that defined as second-generation calcite by Harris (1982) and Kaufman et al. (1988). Sample HP-4-GR.

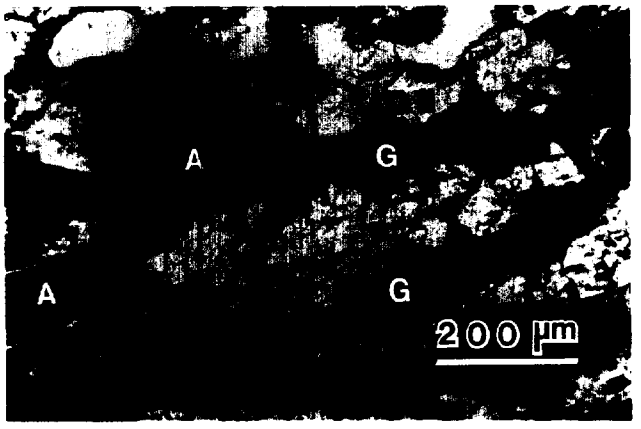

FIG. 5.—Glauconite formation postdating dolomitization. Dolostone comprising dolomite II (DII) rhombs, biogenic apatite (A), and glauconite (G). Anhedral glauconite fills fractures that appear to postdate dolomitization based upon jigsaw fit of rhombs across fracture below DII label. Stratigraphic up is to the top of the photograph. Note fracturing and displacement of originally single-fish apatite fragment. Plane-polarized light. Sample OL-8.9-J, Ollie Quarry, Keokuk County, Iowa.

duller luminescence (and therefore probably has higher Fe concentrations) relative to the remainder of the rhomb (Fig. 3c). Similarly, glauconite inclusions in calcite cement can be restricted to a particular luminescent zone (Fig. 4), suggesting that the glauconite formed during the growth of that cement zone, or the glauconite inclusions can be more randomly oriented within the cement crystal, which may indicate that early-formed glauconite was encased by later calcite.

Fine-grained glauconite crystals also fill interrhombic porosity (Fig. 5), similar to the moldic glaucoliths in calcite cements from the middle Cambrian of southern Baltoscandia described by Berg-Madsen (1983). As discussed by Berg-Madsen, the calcite could postdate the glauconite and grow displacively into a pellet, or the glauconite could have filled voids after calcite cementation. In Burlington-Keokuk dolostones, the presence of glauconite in small interrhomb pores with openings to larger pore spaces that are not glauconite-filled suggests that some of this form of glauconite crystallized from a fluid after the formation of the dolomite (Fig. 3). If the pellets, which are typically five times as large as the rhombs, were displaced into the remaining pore space during dolomite growth, then all sizes of pores should have portions of displaced pellets in them.

Glauconite occurs in fractures and stylolites that are lined with dolomite and calcite cements, and its formation must postdate or be contemporaneous with these features. In the sample shown in Figure 6, for example, a fracture through a crinoid ossicle is lined with calcite cements whose cathodoluminescent zones approximately parallel the length of the fracture. Dolomite II rhombs in

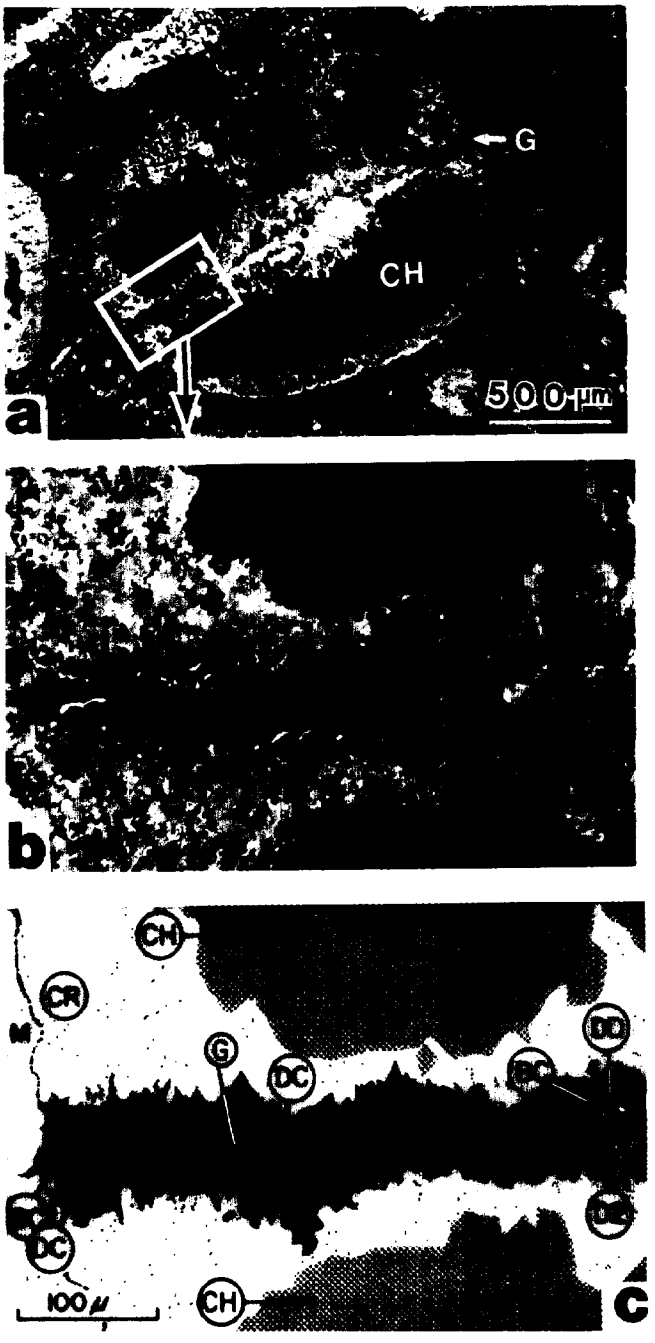

FIG. 6.—Late paragenesis of glauconite. a) Cross section of crinoid ossicle in dolomitized packstone. Replacement of calcite by chert (CH) gives eyes-and-mouth appearance to crinoid. Fracture running the length of cross section is healed on both ends by anhedral glauconite (G). Plane-polarized light. b) Close up of box in (a) under cathodoluminescence with labeled sketch in (c). CH = chert; CR = crinoid calcite; G = glauconite; BC = calcite cement with bright cathodoluminescence; DC = calcite cement with dark cathodoluminescence; D2 = dolomite II; DD = dedolomite calcite; M = dolomitized matrix. Fracture was lined first with dark cement with bright hairlines, characteristic of first-generation calcite cement (Harris 1982; Kaufman et al. 1988). Dedolomitization was contemporaneous with this cementation episode, as indicated by the identical luminescence of the bright calcite lining the fracture and replacing dolomite II. Glauconite filled the remaining pore space in the fracture and therefore postdates dolomitization, cementation, and dedolomitization. Sample N-3, Nelson Quarry, Des Moines County, Iowa.

TABLE 1.—*Electron microprobe analyses of glauconite pellets from a glauconite-poor (GF) and adjacent glauconite-rich (GR) horizon, Burlington-Keokuk Fm., Harper Quarry, Iowa. Sample HP-4. Total Fe as FeO. a, b refer to core and rim analyses of the same pellet*

Wt.%	GF1a	GF1b	GF2	GF3a	GF3b	GR1	GR2	GR3a	GR3b	GR4	GR5	GR6	GR7
SiO_2	53.8	54.0	53.6	48.5	51.1	49.6	50.7	50.8	51.6	51.0	52.9	50.6	52.2
Al_2O_3	9.9	10.2	12.0	10.8	9.5	9.8	10.7	10.2	12.5	9.8	10.7	9.3	11.4
FeO	17.2	16.7	14.1	13.7	16.5	16.8	15.2	16.6	14.2	16.8	16.0	16.6	15.5
MgO	4.6	4.4	4.3	4.0	4.3	4.5	4.8	4.6	4.6	4.6	4.6	4.6	4.5
CaO	0.1	0.2	0.2	0.2	1.3	0.1	0.3	0.2	0.3	0.1	0.2	0.1	0.2
Na_2O	0.1	0.1	0.2	0.1	0.1	0.1	0.2	0.1	0.1	0.1	0.1	0.1	0.1
K_2O	9.2	9.4	9.0	7.8	9.2	8.8	9.0	9.1	9.0	9.0	9.2	9.3	9.1
SUM	94.9	95.0	93.3	85.0	92.0	89.7	90.8	91.6	92.1	91.6	93.7	90.6	93.0

this fracture are partially dedolomitized by these cements. Glauconite heals this fracture on both ends at the perimeter of the crinoid and thus postdates dolomitization, calcite cementation, and dedolomitization. Glauconite in stylolite seams has a range of morphologies which varies from accumulations of insoluble pellets to more finely crystalline glauconite which fills in the seams. The latter form suggests that glauconite was recrystallized during pressure solution.

Limited electron microprobe analyses indicate that glauconites in the different occurrences have distinct compositions. Pellets from a glauconite-rich and glauconite-poor horizon in the Burlington-Keokuk Fm. show an inverse correlation between total iron (as FeO) and Al_2O_3 content (Table 1). Similar variations in Cambrian and recent glauconites are attributed to substitution of iron for aluminum during recrystallization (Berg-Madsen 1983; Bornhold and Giresse 1985). The limited analyses on Burlington-Keokuk glauconite pellets indicate that they have uniform MgO (4.0–4.8 wt.%) and K_2O (7.8–9.4 wt.%) contents. The MgO and K_2O contents are also at the high end of the range of values reported in the literature for glauconites from nine other localities and ages (Odin and Mater 1981). Variations in these parameters have been ascribed to the effects of sedimentation patterns and source regions (Berg-Madsen 1983).

Reaction between postdepositional diagenetic fluids and glauconite may be important in the geochemical evolution of the glauconite. Glauconite inclusions in dolomite and calcite can be restricted to duller cathodoluminescent zones, suggesting that relatively iron-rich (or reducing) diagenetic fluids formed both glauconite and carbonate. The interstitial glauconite occurrences that postdate dolomitization and calcite cementation have higher H_2O contents and a larger smectite component compared to the pellets (Bartholomew et al. 1987). These hydrous compositions are characteristic of relatively immature glauconite (Odin and Mater 1981), consistent with its proposed late formation.

Rare earth element patterns of glauconite pellets separated from Burlington-Keokuk dolostones have low chondrite-normalized Ce/Nd ratios (i.e., negative cerium anomalies), indicative of a seawater source for the rare earth elements in the pellets (Banner et al. 1988b). This is consistent with an authigenic marine origin for the glauconite. If the glauconite was of detrital origin, the pellets would be expected to have high Ce/Nd ratios and light rare earth element enrichment typical of crustal silicates. Further investigations into glauconite geochemistry within a diagenetic framework may help place independent constraints on diagenetic fluid compositions.

Sample Selection

Plane, reflected, and cathodoluminescent-light petrography were used to select whole-rock dolostones that are composed of nearly pure dolomite of greater than 90 percent of one cathodoluminescent type (Table 2). Some nondolomite impurities are present in all samples. The samples characterized as nearly pure have less than one percent of glauconite and less than five percent total of other phases such as calcite, chert, sulfides, oxides, and apatite. Some finely crystalline material, presumably clay minerals, is anhedral and submicroscopic (less than 1 μm), which precludes accurate identification and estimation of their contents in the nearly pure dolostones. Qualitative electron microprobe analysis indicates that some of this material is an Fe silicate. The total noncarbonate fractions of these dolostones, as determined by insoluble residue contents measured on selected whole-rock samples are less than or equal to five percent. For some dolostones with significant amounts of nondolomite phases, mineral separates were obtained and the purified dolomite portions were analyzed. In order to determine the effects of the nondolomite phases on the isotopic analyses, a sequence of dissolution experiments was conducted to 1) dissolve ideally only the carbonate portion of a sample and 2) dissolve the entire sample.

ANALYTICAL METHODS

All whole-rock samples were ground to less than 200 mesh. Mineral separates were prepared using ultrasonic disaggregation, heavy liquids, a Franz magnetic separator, hand picking, and settling columns. Approximately 200-mg splits of sample powders were treated separately by three different methods of dissolution using covered teflon beakers and stir bars.

1) Samples were leached in 1.25N HCl at 50°C for 30 minutes with stirring. All observable reaction of carbonate occurred under these conditions. For the nearly pure dolostones analyzed in this study, it was found that even small percentages of nondolomite contaminants made

TABLE 2.—*Comparative dissolution analyses of Sr isotopic compositions and Rb and Sr concentrations for Burlington-Keokuk dolomites and associated phases*

Sample	$^{87}Sr/^{86}Sr_m$		Rb, ppm		Sr, ppm		$^{87}Rb/^{86}Sr$	$^{87}Sr/^{86}Sr_i$
	Leach	Complete Dissolution	Leach	C.D.**	Leach	C.D.	C.D.	C.D.
Dolomite I								
1	0.70777 ± 3	0.70812 ± 3	0.74	1.252	112.3	110.2	0.0329	0.70796
Replicate	—	0.70807 ± 4	—	1.237	—	108.1	0.0331	0.70791
	0.70795 ± 3*	—	—	—	—	—	—	—
2	0.70777 ± 3	0.70826 ± 4	1.58*	1.493	111.4*	103.8	0.0416	0.70806
3	—	0.70782 ± 4	—	0.417	—	108.0	0.0112	0.70777
4	0.70897 ± 7	0.70902 ± 5	2.72	8.26	123.9	123.3	0.194	0.70808
Replicate	0.70799 ± 3	—	—	—	—	—	—	—
	—	—	7.93*	—	123.7*	—	—	—
5	0.70801 ± 4	0.70857 ± 4	2.79	7.57	107.5	106.6	0.205	0.70757
Replicate	—	—	1.83	—	105.6	106.7	—	—
6	0.70802 ± 4	0.70818 ± 7	—	2.61	107.3	118.3	0.0638	0.70787
7	0.70808 ± 3	—	—	—	106.6	—	—	—
Dolomite II								
8	0.70943 ± 4	0.71170 ± 4	2.48	8.68	54.8	53.7	0.468	0.70942
Replicate	—	0.71168 ± 5	—	8.84	—	54.4	0.470	0.70939
9	0.71033 ± 3	0.71023 ± 5	2.55*	4.46	34.7*	53.5	0.241	0.70906
Replicate	—	0.71020 ± 3	—	4.46	—	52.4	0.246	0.70900
10	0.70905 ± 4	0.71044 ± 5	4.90*	4.82	54.6*	54.2	0.257	0.70919
11	0.70949 ± 4	0.70993 ± 4	2.03*	2.19	49.9*	49.9	0.127	0.70931
Replicate	—	—	—	2.18	—	49.7	0.127	—
12	0.70977 ± 4	0.71049 ± 3	—	5.10	58.8*	50.8	0.290	0.70908
13	—	0.70929 ± 6	—	1.98	—	62.9	0.0911	0.70885
Dolomite II'								
14	0.71092 ± 4*	0.71111 ± 4	—	6.46	53.0*	53.2	0.351	0.70940
15	0.71216 ± 4*	0.71219 ± 4	15.02*	12.44	55.7*	59.7	0.603	0.70925
	0.71032 ± 9	—	—	—	—	—	—	—
Replicate	0.71062 ± 9	—	—	—	—	—	—	—
Vug Carbonates								
16 Dolomite	0.71024 ± 3	—	0.452	—	91.3	—	—	—
17 Calcite	0.70986 ± 4	0.70987 ± 5	—	0.043	—	87.1	0.00143	0.70986
Oxide-clay-rich dolostone								
18	0.70890 ± 3	0.71739 ± 4	35.1*	40.9	79.3*	72.3	1.64	0.70941
Replicate	—	0.71735 ± 7	—	—	—	74.0	—	—
Biogenic Apatites								
19	0.70890 ± 4	—	6.98	—	1,406	—	—	—
20	0.70897 ± 3	0.70899 ± 4	—	2.78	—	1,409	0.00571	0.70896

Leach analyses refer to HCl leaching (method 1 in text), except analyses denoted by *, which refer to HCl + HF leaching (method 2). **, C.D. = complete dissolution (method 3). —, not determined. $^{87}Sr/^{86}Sr_m$ = measured $^{87}Sr/^{86}Sr$ ratio. Initial $^{87}Sr/^{86}Sr$ ratio = $^{87}Sr/^{86}Sr_i = {}^{87}Sr/^{86}Sr_{measured} - {}^{87}Rb/^{86}Sr(e^{\lambda T} - 1)$, calculated for 342 Ma. Quoted uncertainties are at the two-sigma level for the last digit shown. λ = Decay constant for $^{87}Rb = 1.42 \times 10^{-11}yr^{-1}$. Sample key: except where noted otherwise, samples are whole-rock dolostones as described in text. Detailed petrographic descriptions, sample localities, and stratigraphic positions are given in Banner (1986) and may be obtained from the authors. Dolomite I: (1) MD-F; (2) DH-8; (3) DH-8DS = Dolomite separate from whole rock; (4) HP-18-J; (5) BV-11; (6) BV-6.8-JGFDS = Dolomite separate from whole rock; (7) BV-6.8-JGRDS = Dolomite separate from glauconite-apatite-rich whole rock. Dolomite II: (8) HP-3-J; (9) HP-10.1-J; (10) KS-8; (11) DC-18; (12) MPA-2; (13) HP-4-GFDS = Dolomite separate from whole rock; (14) DC-23; (15) HP-15-J. Vug Dolomite: (16) GR-F-1. Vug Calcite: (17) GR-6cc. (18) PL-J-22 = Iron oxide clay-rich dolostone. (19) BV-F = Apatite separate from chondricthyan finspine. (20) HP-F = Apatite separate from ichthyolith tooth.

significant contributions to the analyses. These results are discussed below.

2) Samples were leached with a 30:1 mixture of 1.25N HCl and concentrated HF, respectively, at 50°C for 30 minutes with stirring. This proportion of HF was added to dissolve the small amounts of HCl-insoluble residue. This dissolution procedure in most cases enhanced the noncarbonate contributions to the analyses. However, some residue was visible for some samples after this process.

For methods 1 and 2, leachates were filtered before being added to cation exchange columns. Separate splits of the powdered samples were used for isotope composition and isotope dilution analysis. For isotope dilution analysis, isotopically enriched ^{87}Rb and ^{84}Sr spikes were added to the particular acid prior to dissolution.

3) Samples were completely decomposed by a sequence of dissolutions using concentrated HF and HNO_3 and 6N HCl as follows. Samples were placed in a 10:1 mixture of concentrated HNO_3 and HF in a covered teflon beaker, stirred and then digested at 80°C for 12 hours. After evaporation of the acids, the residue was digested in the same manner in a 5:1 mixture of concentrated HF and 6N HCl. The residue from this step was digested in 6N HCl. The

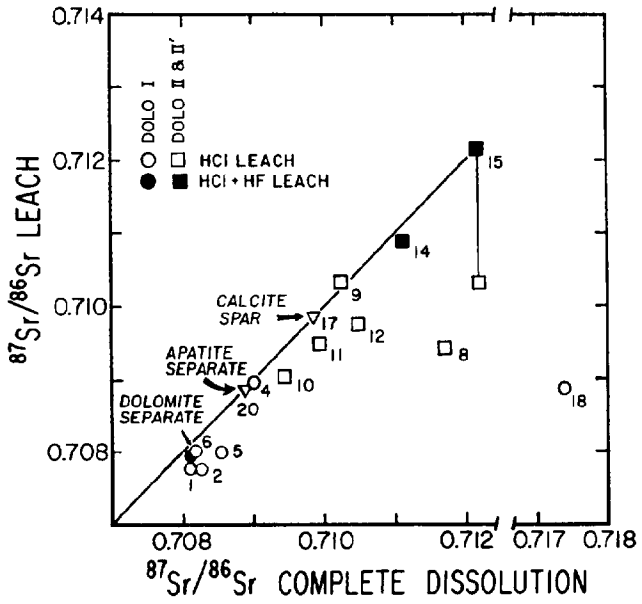

FIG. 7.—$^{87}Sr/^{86}Sr$ ratio determined by acid leaching vs. $^{87}Sr/^{86}Sr$ ratio determined by complete dissolution for Burlington-Keokuk Fm. dolostones, a dolomite separate, an apatite separate, and a calcite spar. Symbols denote different luminescent dolomite types and different leaching agents. Numbers next to data points refer to sample numbers in Table 2.

dissolution sequence was repeated if any undissolved sample remained. The sample solution was divided into aliquots, one of which was spiked for isotope dilution analysis. Isotope composition analyses were made on Sr separated from the unspiked portion.

Rb and Sr separations were carried out with HCl using standard cation exchange procedures. Mean analytical blanks were less than 6 ng for Sr and 1 ng for Rb, resulting in negligible uncertainties for the samples analyzed in this study.

Rb and Sr for isotope dilution analysis were loaded as nitrates on double Re filament assemblies, and ratios were measured on a 15-cm radius of curvature, NBS-design, surface-emission mass spectrometer. Strontium for isotope composition analysis was loaded as a nitrate on a triple Re filament. Ratios were measured on a 30-cm radius of curvature, NBS-design mass spectrometer. Ratios were normalized to a value of $^{86}Sr/^{88}Sr = 0.1194$. Twenty-nine analyses of NBS standard SRM 987 over an eighteen-month period during the course of this study gave a mean value of 0.71034 with a value for one standard deviation of a given analysis of ± 0.00002. Instrumental bias produces variations in the reported values of this Sr standard solution for different laboratories (e.g., 0.71014, Burke et al. 1982; 0.71031, DePaolo and Ingram 1985), and it is essential to account for interlaboratory bias when comparing results from different laboratories.

RESULTS

$^{87}Sr/^{86}Sr$ ratios and Rb and Sr abundances for the three dissolution methods are presented in Table 2. For dolomite I samples, the measured Sr isotopic compositions range from 0.70777 to 0.70897 by the two leaching methods (methods 1 and 2) compared to a slightly higher range of 0.70782 to 0.70903 for the complete dissolution procedure (method 3). Similarly, whole-rock dolomite II samples give ranges of 0.70905 to 0.71216 by leaching and 0.70993 to 0.71219 by complete dissolution. Figure 7 compares these results for each sample and illustrates that the measured $^{87}Sr/^{86}Sr$ ratios for all dolomite types are higher by the complete dissolution method compared to the leaching methods. A clay- and oxide-rich dolostone, sample 18, has the highest $^{87}Sr/^{86}Sr$ ratio by complete dissolution, 0.71739, and the largest difference in results bewteen dissolution methods (0.70890 by HCl leaching). This sample also has a large insoluble residue content of 40 percent.

The dolomite separate from sample 6 gives a slightly higher $^{87}Sr/^{86}Sr$ ratio by complete dissolution than by HCl leaching. Sample 3, the separate from sample 2, gives a lower $^{87}Sr/^{86}Sr$ value by complete dissolution (0.70782) than the whole-rock (0.70826) by complete dissolution and essentially the same value compared to the HCl leach result for the whole-rock (0.70777).

The whole-rock and dolomite separate results demonstrate that relative to HCl, HF more readily dissolves phases with radiogenic ^{87}Sr. Figure 7 also shows that as $^{87}Sr/^{86}Sr$ increases, the difference in values between the dissolution methods increases. Dolomites II and II' have higher values of $^{87}Sr/^{86}Sr$ compared to dolomite I by all methods of dissolution. Leaching and complete dissolution give results within analytical uncertainty for the Sr isotopic composition of the apatite separate and the calcite spar.

Rb concentrations vary from less than 1 to 40.9 ppm in the dolostones and are uniformly higher by complete dissolution compared to HCl leaching (Fig. 8a). A comparison of the HCl leach and complete dissolution data demonstrates that HCl leaching removes from 24–60 percent of the Rb in the samples. HF + HCl leaching gives Rb concentrations ranging from nearly identical to those for complete dissolution to variably higher and lower Rb concentrations relative to complete dissolution analyses. Note that dolomites I and II have the same ranges of Rb concentrations by method 3, in contrast to their distinctly different ranges of $^{87}Sr/^{86}Sr$ ratios and Sr contents. $^{87}Rb/^{86}Sr$ ratios are lowest in the vug carbonates and apatite (< 0.015), and highest in the clay- and oxide-rich dolostone (1.64).

Figure 8b illustrates the narrow range in Sr concentrations for each dolomite type, 104–124 ppm for dolomite I and 50–63 ppm for dolomites II and II'. Sr abundances are less variable between dissolution methods compared to Rb and $^{87}Sr/^{86}Sr$ values. Six of twelve samples give Sr concentrations by the two methods of leaching that are within one percent of the values for the same samples by complete dissolution. The samples that lie outside of this difference show no systematic relationship between Sr concentration and dissolution method. For the two samples (4, 15) that were analyzed by all three methods, methods 2 and 3, which include HF, give more similar results for $^{87}Sr/^{86}Sr$ and Rb than method 1 involving only HCl.

Reproducibility

Complete replicate analyses (Table 2) on separate splits of the same sample powder, including dissolution and chemical separation, show that the complete dissolution method gives significantly more reproducible results than leaching for both isotopic compositions and elemental abundances. Based on replicate analyses of four samples, $^{87}Sr/^{86}Sr$ ratios are reproducible to ± 0.00002 (< 0.003%) by complete dissolution. This is comparable to the precision obtained for repeated analyses of SRM 987. Precision for Rb (four samples) and Sr (six samples) abundances is better than ± 1 percent of the amount present.

Based on replicate analyses for two samples, reproducibility for leach analyses is an order of magnitude lower for $^{87}Sr/^{86}Sr$ values ($\pm$ 0.04%). Rb abundances vary by 60 percent for replication of one sample. Three samples were replicated for Sr abundances by acid leaching and indicate a reproducibility of better than ± 1 percent, similar to the precision achieved by complete dissolution.

DISCUSSION

The results of comparative dissolution experiments indicate that the dolostones contain a minor phase which is an important host for Rb and radiogenic ^{87}Sr. The higher Rb concentrations and $^{87}Sr/^{86}Sr$ values in the HF-soluble portions of the samples, and electron microprobe scans for K indicate that most of the Rb is in the non-carbonate portions of the rocks. The similar Sr concentrations determined by different dissolution methods on the same samples indicate that the dolomite contains nearly all of the Sr.

A silicate mineral such as glauconite, which would be more readily dissolved by HF compared to HCl, has the requisite $^{87}Sr/^{86}Sr$, Rb/Sr ratios and Rb abundances to account for the differences between the leach and complete dissolution values. For example, consider a glauconitic dolostone in which the dolomite and glauconite were in isotopic equilibrium at 342 Ma ($^{87}Sr/^{86}Sr = 0.7079$) and which is composed of 1) four percent glauconite with 230 ppm Rb and 5.5 ppm Sr (based on data from Grant et al. 1984), which would have a present-day $^{87}Sr/^{86}Sr$ ratio of 1.3329; and 2) 96 percent dolomite I with 1 ppm Rb, 110 ppm Sr, and $^{87}Sr/^{86}Sr = 0.7080$). These constituents give a whole-rock composition of $^{87}Sr/^{86}Sr = 0.7092$, 10.2 ppm Rb, and 106 ppm Sr. The glauconite contains only 0.2 percent of the total Sr but 92 percent of the radiogenic ^{87}Sr in the sample. Owing to the high Rb and low Sr abundances in glauconite, physical mixtures of dolomite I and less than four percent glauconite will yield whole-rock $^{87}Sr/^{86}Sr$ ratios equivalent to the range observed for dolomite I whole-rock samples. These percentages are smaller than the insoluble residue contents determined on selected samples and greater than the less than one percent modal clay observed, indicating that submicroscopic clays with high concentrations of Rb and radiogenic ^{87}Sr may account for the observed data.

In order to constrain petrogenetic models, it is essential to determine the isotopic composition of a diagenetic phase at the time of its formation. The relatively high Rb/Sr ratios of the Burlington-Keokuk dolostones necessitate an age correction of each sample's measured Sr isotopic composition. Owing to the uncertainties inherent in the leaching results, in terms of clay-site selectivity (Thompson and Hower 1973) and analytical reproducibility, initial $^{87}Sr/^{86}Sr$ ratios are determined for Burlington-Keokuk dolostones using analyses by complete dissolution (Fig. 9; Table 2).

The numbered lines in Figure 10 portray the change of $^{87}Sr/^{86}Sr$ with time for each dolostone and dolomite sep-

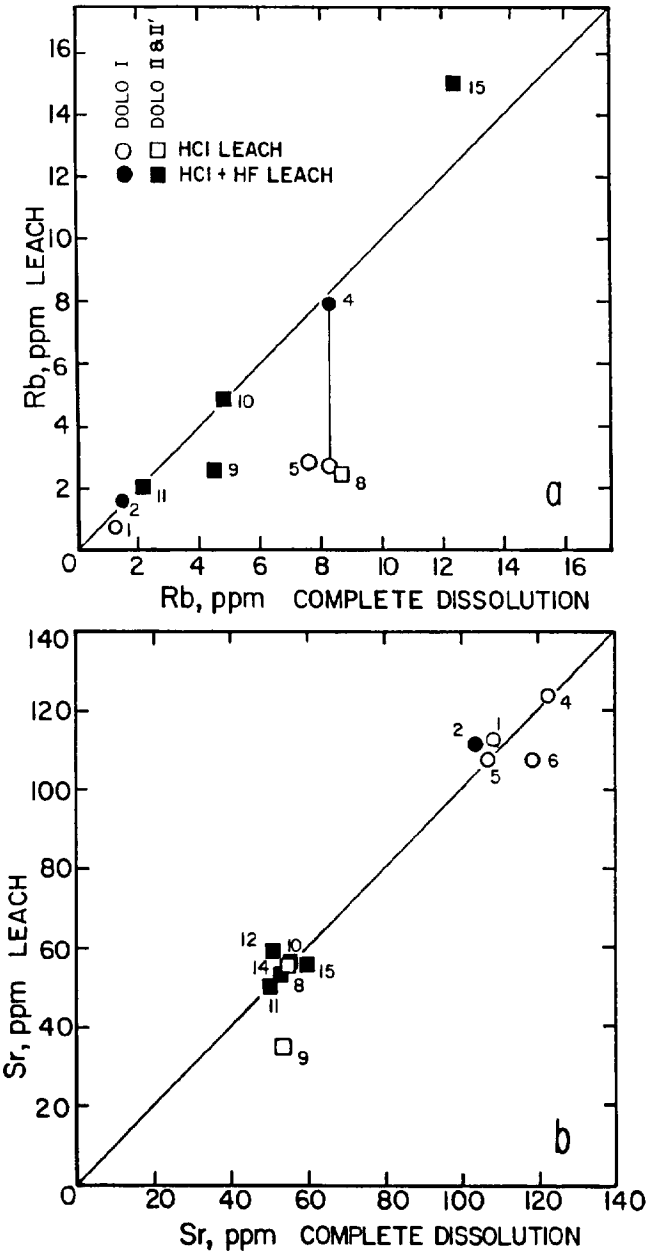

FIG. 8.—a) Comparison of Rb concentrations (ppm) determined by acid leaching and complete dissolution, and b) the same comparison for Sr concentrations. Symbols as in Figure 7.

arate.This figure illustrates the effect of the uncertainty on the timing of dolomite formation on the calculated initial ratios. For example, the youngest age estimate of pre-Early Permian for dolomites II and II′ corresponds to an increase of less than or equal to 0.0003 in the initial $^{87}Sr/^{86}Sr$ ratio for most dolomite II and II′ samples, with a maximum difference of 0.0005 for sample 15 with the highest $^{87}Rb/^{86}Sr$ ratio (0.6). Most petrographic evidence points to an age range of 342–320 Ma for dolomite II formation, corresponding to a difference of less than 0.0001 in the calculated initial ratio for most samples. The oldest age estimate for dolomites II and II′ corresponds to the narrowest range of initial $^{87}Sr/^{86}Sr$ ratios for this group of samples. The Sr isotope evolution diagram (Fig. 10) shows the significant differences between the uncorrected ratios ($T = 0$ Ma) and the initial $^{87}Sr/^{86}Sr$ ratios, demonstrating the importance of 1) the determination of Rb and Sr abundances and 2) age constraints on diagenesis for determining the Sr isotopic compositions of the dolomites at the time of their formation.

Origin and Diagenetic History of Clay Components: Implications for Rb-Sr Exchange and Effects on Initial $^{87}Sr/^{86}Sr$ Ratios

Using the isotopic composition and elemental abundances obtained on whole-rock samples to calculate initial $^{87}Sr/^{86}Sr$ ratios for a given dolomite assumes that the Rb- and Sr-bearing phases in a given sample were in isotopic equilibrium at the time of dolomite formation and remained closed to Rb and Sr exchange. The origin and diagenetic history of the clay component of a dolostone is critical in determining its contribution to the whole-rock analysis:

1) An authigenic clay mineral and dolomite that crystallized at the same time from the same fluid and remained undisturbed to the present would have identical initial $^{87}Sr/^{86}Sr$ ratios. A whole-rock sample comprising this carbonate and clay would also have the same initial $^{87}Sr/^{86}Sr$ ratio.

2) Detrital clays would most likely have been derived from source regions that are on average older than 1.0 AE, based on sedimentological and Nd isotopic studies of the Burlington-Keokuk carbonates and penecontemporaneous clastic sediments (Lineback 1968; Banner et al. 1988b). Such minerals might have had quite high $^{87}Sr/^{86}Sr$ ratios relative to seawater at 342 Ma. Therefore, calculation of an initial $^{87}Sr/^{86}Sr$ ratio for 342 Ma for a carbonate rock containing detrital clay would yield an incorrect and high initial ratio for the carbonate phase.

3) If the fluids that formed dolomites I and II also exchanged Rb and Sr with either authigenic or detrital clay minerals, the clays would be transformed toward isotopic equilibrium with the dolomites at the time of dolomitization. If transformation is complete, then the clay and dolomite would have identical initial $^{87}Sr/^{86}Sr$ ratios.

The results of Rb-Sr geochronologic studies of glauconite and illite indicate that 1) the interlayer cation site in the phyllosilicate structure readily exchanges Rb and Sr with diagenetic fluids, and 2) complete recrystallization of clays can occur during diagenesis (Grant et al. 1984; Morton and Long 1983; Kralik 1984; Morton 1985).

Grant et al. (1984) immersed glauconite pellets in fluids of different Sr isotopic compositions and Rb and Sr concentrations. They found that the glauconite exchanged Sr to the extent that the $^{87}Sr/^{86}Sr$ ratio of the glauconite began to approach the fluid $^{87}Sr/^{86}Sr$ ratio within days. This exchanged Sr resisted subsequent leaching with ammonium acetate. These experimental results suggest that glauconite Rb-Sr systematics can be reset by diagenetic fluids and that this process may be irreversible in some instances.

The petrographic and geochemical features of glauconite in the Burlington-Keokuk rocks indicate that it is an authigenic phase and that at least some exchange of components between glauconite and fluid took place during dolomitization. The common occurrence of nonpelletoidal glauconite morphologies in rocks with abundant (> 5%) glauconite pellets suggests that remobilization of glauconite on a local scale occurred in association with influxes of diagenetic fluids. This newly formed (dispersed) glauconite probably formed in Sr isotopic equilibrium with the diagenetic fluids. In light of the ease with which glauconite appears to exchange interlayer Rb and Sr with diagenetic fluids and the pervasive nature of the major episodes of diagenesis in the Burlington-Keokuk Fm., interlayer exchange of Rb and Sr may have occurred between diagenetic fluids and the unrecrystallized (pelletoidal) glauconite in a sample.

Diagenetic carbonates that are precipitated from the same fluids which completely exchange with or transform clay phases will have the same initial $^{87}Sr/^{86}Sr$ ratio as the clay. Therefore, initial isotope ratios for carbonates may be determined on whole rocks with such transformed or exchanged clay components. Figure 11 graphically illustrates this for a hypothetical sample (Whole-Rock A), for which all constituent phases formed at 342 Ma. This example was described earlier, in which the dolomite, glauconite, and whole rock have identical $^{87}Sr/^{86}Sr$ ratios at 342 Ma and widely divergent present-day Sr isotopic compositions.

The petrographic constraints cannot be used to time the dolomite and clay in a dolostone to have formed at precisely the same time, and such uncertainties translate into errors on dolomite initial $^{87}Sr/^{86}Sr$ ratios. However, the petrography can place reasonable limits on absolute ages. These limits are used here to demonstrate that since the major episodes of diagenesis occurred within a relatively short time after deposition of the Burlington-Keokuk Fm., the formation of dolomite and glauconite at different times and from different fluids during this interval will not significantly affect dolomite initial $^{87}Sr/^{86}Sr$ ratios determined from whole-rock analyses. Figure 11 displays the uncertainties that would be associated with estimating initial $^{87}Sr/^{86}Sr$ ratios for the dolomite from measurements on five hypothetical whole-rock samples that are composed of A) dolomite and glauconite which formed at the same time and from the same fluid;

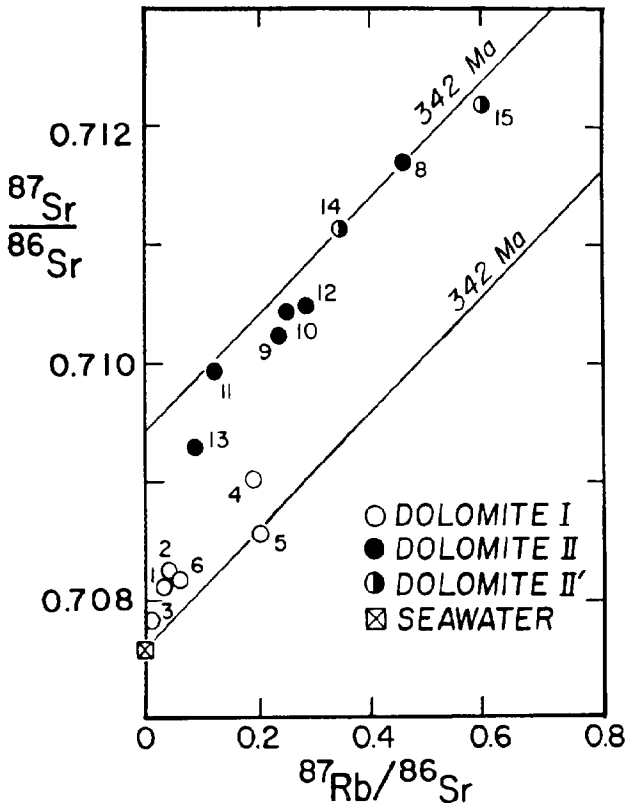

FIG. 9.—$^{87}Sr/^{86}Sr$ vs. $^{87}Rb/^{86}Sr$ for the major dolomite types in the Burlington-Keokuk Fm. as determined by complete dissolution. Reference lines of 342 Ma are plotted through an individual dolomite II point and through the value for Osagean seawater to illustrate extrapolation to initial $^{87}Sr/^{86}Sr$ ratios on y-axis. Seawater value from Kaufman et al. (1986).

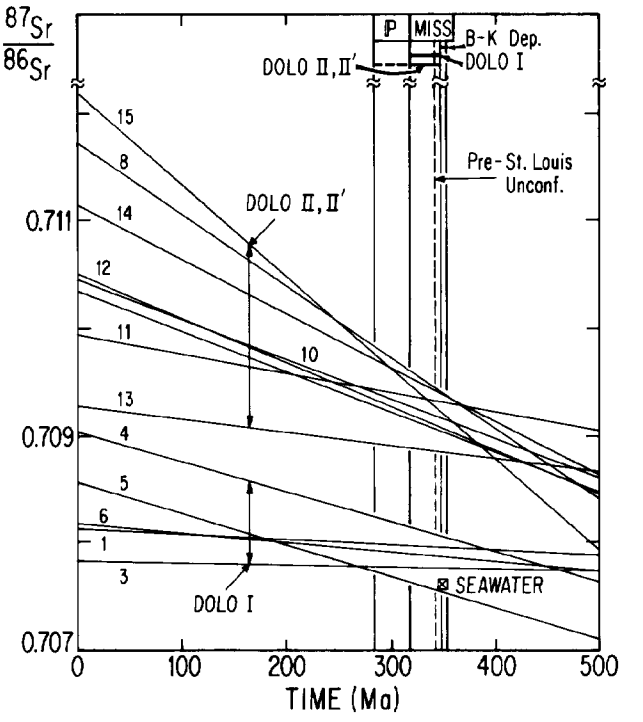

FIG. 10.—Sr isotope evolution of the major dolomite types in the Burlington-Keokuk Fm. as determined by complete dissolution. Each sample has a unique trajectory (numbered as in Table 2) in $^{87}Sr/^{86}Sr$ vs. time space, with slopes proportional to Rb/Sr. Limits of age constraints on dolomite formation shown as defined by regionally correlative zonal stratigraphies of calcite and dolomite based on cathodoluminescence and the relationship between the zonal stratigraphies and younger stratigraphic rock units, as discussed in text. Note large differences in absolute values and range of values of uncorrected $^{87}Sr/^{86}Sr$ ratios (T = 0 Ma) and calculated initial ratios.

B) I—authigenic marine glauconite and dolomite I which formed 38 Ma after the glauconite (seawater $^{87}Sr/^{86}Sr$ = 0.7076); II—authigenic marine glauconite and dolomite II which formed 30 Ma later from a fluid with $^{87}Sr/^{86}Sr$ = 0.7090; C) Mississippian dolomite I and authigenic glauconite which formed 38 Ma after the dolomite from a fluid with $^{87}Sr/^{86}Sr$ = 0.710; and D) detrital illite from a 1,500 Ma old crustal source and Mississippian dolomite I. In each case, an age of 342 Ma was used to calculate initial ratios for the whole rock, regardless of the age of the individual phases.

The results of the calculations in Figure 11 show that for cases A and B (I and II), the whole rock gives an indistinguishable initial $^{87}Sr/^{86}Sr$ ratio compared to the actual dolomite initial ratio. In case C, the whole-rock initial is lower than the actual dolomite initial by 0.0001, slightly outside the analytical uncertainty. This indicates that if the glauconite and dolomite in a sample formed at different times greater than 30 Ma apart, the calculated initial for the whole rock may significantly deviate from the actual dolomite initial. Since the glauconite contains such large abundances of Rb relative to the dolomite, four percent glauconite formed within ±30 Ma of the dolomite will eventually develop over 90 percent of the radiogenic ^{87}Sr in the sample. However, during the time interval in which the dolomite and glauconite form, the radiogenic ^{87}Sr content is minor compared to the total Sr in the rock. Case D shows that detrital clays will give erroneously high initial $^{87}Sr/^{86}Sr$ ratios for the whole-rock method.

Thin, shaly carbonate horizons in the Burlington-Keokuk Fm. have a significant detrital silicate component, based on rare earth element patterns with relatively high Ce/Nd ratios and high initial $^{87}Sr/^{86}Sr$ ratios of up to 0.714 (Banner et al. 1988b; Chyi et al. 1985). More finely dispersed, submicroscopic clays of detrital origin are probably also present in small amounts in the nearly pure carbonates analyzed in this study. Such fine-grained clays can be isotopically transformed during diagenesis (Morton 1985), such that retention of original detrital Rb and Sr may be insignificant relative to the sum of original authigenic plus transformed or exchanged Rb and Sr in the dolostones. Thus, potential uncertainties in the calculated initial $^{87}Sr/^{86}Sr$ for the dolostones include 1) the presence of a significant detrital component in the clay within a sample, and 2) reequilibration of clay or carbonate with post-Pennsylvanian diagenetic fluids.

Another potential uncertainty is the presence of more

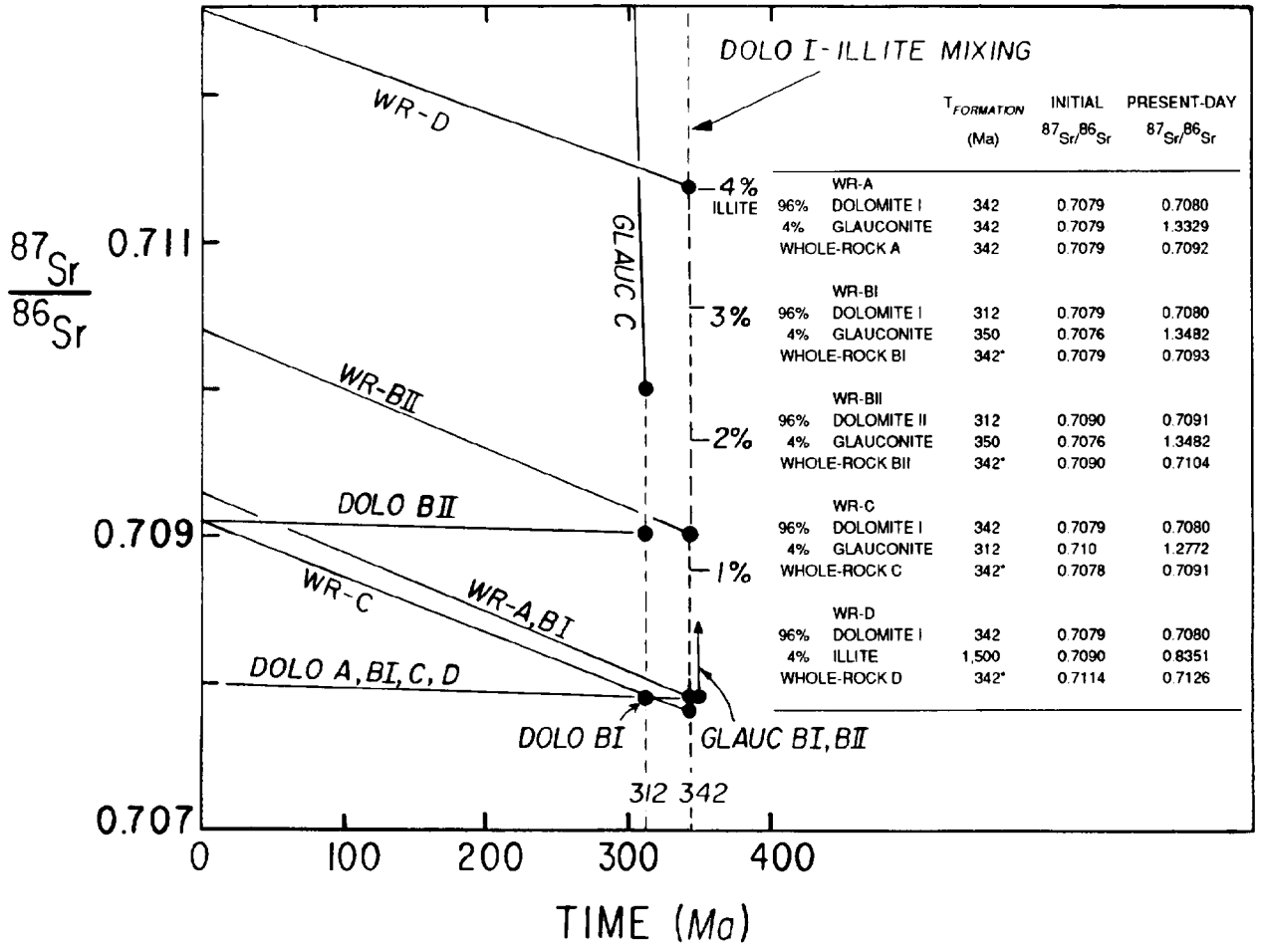

FIG. 11.—Sr isotope evolution pathways for five hypothetical whole-rock dolostone samples (WR-A, -BI, -BII, -C, -D), illustrating effects of carbonate and clay diagenetic histories on calculated whole-rock initial $^{87}Sr/^{86}Sr$ ratios. A) Coeval dolomite and glauconite; B) I—dolomite I formation postdating authigenic marine glauconite formation, II—dolomite II formation postdating authigenic marine glauconite formation; C) postmarine glauconite formation postdating dolomite I formation; and D) mixing of detrital illite and dolomite I. See text for diagenetic fluid Sr isotopic compositions. Compare calculated whole-rock initial $^{87}Sr/^{86}Sr$ ratios with actual dolomite initial $^{87}Sr/^{86}Sr$ ratios for each sample. The following concentrations were used: Dolomite: 1 ppm Rb, 110 ppm Sr (this study). Glauconite: 230 ppm Rb, 5.5 ppm Sr (Grant et al. 1984). Illite: 200 ppm Rb, 100 ppm Sr (Kralik 1984). * Denotes age used for calculating initial $^{87}Sr/^{86}Sr$ ratio for whole rock with noncoeval phases. In all other instances, $T_{formation}$ was used to calculate initial $^{87}Sr/^{86}Sr$ ratios. All initial ratios shown as filled symbols. Vertical dashed line at 342 Ma illustrates whole-rock mixtures of dolomite I and 1, 2, 3, and 4% detrital illite. Glauconite A trajectory not shown for clarity.

than one cathodoluminescent dolomite type with distinct isotopic compositions in each sample. However, the data for the samples do not lie along a dolomite I–dolomite II mixing curve in $(^{87}Sr/^{86}Sr)_i$ vs. Sr (ppm) space. The narrow range of Sr concentrations for six of eight dolomite II and II′ samples (50–55 ppm) represents a range of less than 10 percent of a dolomite I component in such a mixture, in accord with petrographic observations. Dolomite I samples show a trend of increasing initial $^{87}Sr/^{86}Sr$ ratios with increasing Sr concentrations (Table 2), the inverse of the trend expected for dolomite I–dolomite II mixing.

A comparison of uncorrected leach $^{87}Sr/^{86}Sr$ values with calculated initial $^{87}Sr/^{86}Sr$ ratios for complete dissolutions for the same dolostone samples shows that for several samples, HCl leaching gives significantly higher values compared to calculated initial $^{87}Sr/^{86}Sr$ ratios (Fig. 12). This is a likely consequence of the leaching of radiogenic ^{87}Sr from the clay fractions of these samples. The lower initial $^{87}Sr/^{86}Sr$ ratios compared to the HCl leach values is consistent with the proposed authigenic origin of the glauconite in the dolostones.

For a few samples, leach analysis gives a slightly lower value than the initial $^{87}Sr/^{86}Sr$ ratio. This indicates the presence of small amounts of an HCl-insoluble diagenetic or detrital phase with a relatively high $^{87}Sr/^{86}Sr$ in the dolostones. For example, sample 2, a dolomite I sample, gives an $^{87}Sr/^{86}Sr$ ratio of 0.70777 by leaching and an initial $^{87}Sr/^{86}Sr$ ratio of 0.70806 by complete dissolution. The dolomite separate from this rock (sample 3) gives an

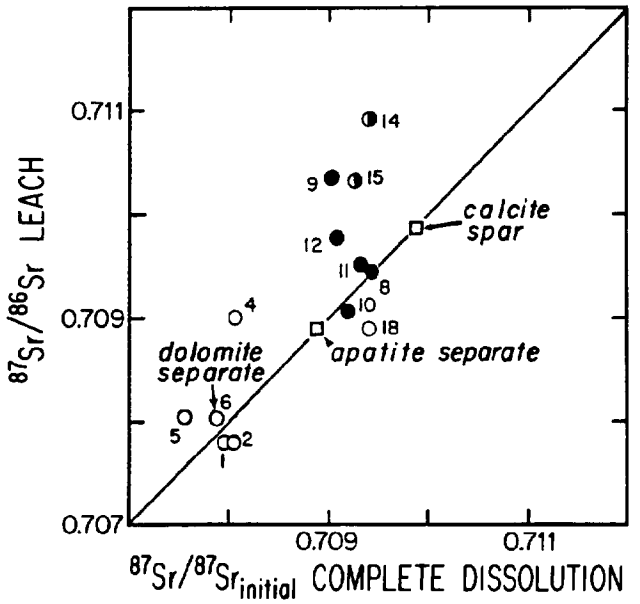

FIG. 12.—Comparison of uncorrected measured $^{87}Sr/^{86}Sr$ ratios by HCl leaching (and HCl + HF leaching for sample 14) and calculated initial $^{87}Sr/^{86}Sr$ ratios by complete dissolution. Symbols as in Figure 9.

initial $^{87}Sr/^{86}Sr$ ratio of 0.70777, identical to the value obtained on the leach of the whole rock. These results suggest that an HCl-insoluble phase, most likely a clay mineral, contains Sr with a significantly higher initial $^{87}Sr/^{86}Sr$ ratio than the dolomite. Similarly, a clay and iron oxide-rich dolomite I dolostone (sample 21) with a high insoluble residue content of 40 percent, also gives a less radiogenic leach value (0.70890) compared to the calculated initial ratio (0.70941). Further investigations using mineral separates and evaluations of different leaching techniques are needed in order to establish precisely the distribution of Rb, Sr, and Sr isotopes among the silicate and carbonate phases in dolostones.

It is unlikely that detrital phases play an important role in determining the initial $^{87}Sr/^{86}Sr$ ratios of the nearly pure whole-rock samples and dolomite separates analyzed in this study. For example, the elevated initial $^{87}Sr/^{86}Sr$ ratios for dolomite I, II, and II′ samples relative to the seawater value cannot be explained by physical mixtures of marine carbonate Sr and detrital Sr during Mississippian time. The narrow range of initial $^{87}Sr/^{86}Sr$ ratios for each dolomite generation compared to their ranges in $^{87}Rb/^{86}Sr$ ratios precludes such a relationship and indicates that the two major dolomite generations formed in isotopically distinct diagenetic environments.

CONCLUSIONS

1) Dolostones of the Burlington-Keokuk Fm. are composed of two major types of dolomite that can be distinguished on petrographic, compositional, and temporal bases. Petrographic and geochemical evidence points to an authigenic, and in some instances a nonmarine, origin for glauconite, the predominant clay mineral in the dolostones.

2) Complete sample dissolution yields significantly higher and more reproducible $^{87}Sr/^{86}Sr$ ratios and Rb abundances compared to acid leaching with HCl or HCl + HF. Leaching with 1.25N HCl appears to remove substantial amounts of Rb and Sr from the small ($\leq$ 5%) fractions of clay in the dolostones. The relatively high Rb/Sr ratios of the dolostones require an age correction for each sample's $^{87}Sr/^{86}Sr$ ratio.

3) Initial $^{87}Sr/^{86}Sr$ ratios are calculated for the dolostones based on estimated ages for the dolomites from regional cathdodoluminescent zonal stratigraphies for calcite and dolomite, and the inference that the detrital component in the clay is negligible. Calculated initial $^{87}Sr/^{86}Sr$ ratios for the samples are significantly different from their present-day $^{87}Sr/^{86}Sr$ ratios by any of the dissolution methods. This demonstrates that a) constraints on the timing and diagenetic history of both the clay and carbonate phases, and b) Rb and Sr analyses are both critical for determining the isotopic composition of the dolomites at the time of their formation.

4) Samples representing each major dolomite generation have a narrow range of initial $^{87}Sr/^{86}Sr$ ratios: 0.70757 to 0.70808 for the earlier dolomite I, and 0.70885 to 0.70942 for dolomites II and II′, preserving isotopic signatures of distinct environments of dolomitization.

ACKNOWLEDGMENTS

Constructive comments by P. J. Hamilton, R. H. McNutt, an anonymous reviewer, K. R. Cercone, M. Kralik, R. J. Reeder, D. A. Sverjensky, and B. W. Ward improved the manuscript. J. M. Budai and P. Bartholomew graciously provided some of the microprobe analyses, and V. Reiger carefully sketched the photomicrographs. This research was supported by grants from the Petroleum Research Fund of the American Chemical Society (PRF 14913AC2) and the Department of Energy (DE-AC02-83ER13112).

REFERENCES

AHARON, P., SOCKI, R. A., AND CHAN, L., 1987, Dolomitization of atolls by seawater convection flow: Test of a hypothesis at Niue, South Pacific: Jour. Geol., v. 95, p. 187–204.

BANNER, J. L., 1986, Petrologic and geochemical constraints on the origin of regionally extensive dolomites of the Burlington-Keokuk Fm., Iowa, Illinois, and Missouri [Ph.D. dissert.]: Stony Brook, State Univ. of New York, 368 p.

BANNER, J. L., HANSON, G. N., AND MEYERS, W. J., 1988a, Water-rock interaction history of regionally extensive dolomites of the Burlington-Keokuk Fm.: Isotopic evidence, *in* Shukla, V., and Baker, P. A., eds., Sedimentology and Geochemistry of Dolostones: Soc. Econ. Paleontologists Mineralogists, Spec. Publ. 43, in press.

BANNER, J. L., HANSON, G. N., AND MEYERS, W. J., 1988b, Rare earth element and Nd isotopic variations in regionally extensive dolomites from the Burlington-Keokuk Fm. (Miss.): Implications for REE mobility during carbonate diagenesis: Jour. Sed. Petrology, in press.

BARTHOLOMEW, P. R., MEYERS, W. J. AND HANSON, G. N., 1987, Glauconite as a geochemical indicator: Geol. Soc. America Abstr. w. Progr., v. 19, p. 581.

BERG-MADSEN, V., 1983, High-alumina glaucony from the middle Cam-

brian of Oland and Bornholm, southern Baltoscandia: Jour. Sed. Petrology, v. 53, p. 875–893.

BORNHOLD, B. O., AND GIRESSE, P., 1985, Glauconitic sediments on the continental shelf off Vancouver Island, British Columbia, Canada: Jour. Sed. Petrology, v. 55, p. 653–664.

BURKE, W. H., DENISON, R. E., HETHERINGTON, E. A., KOEPNICK, R. B., NELSON, H. F., AND OTTO, J. B., 1982, Variation of seawater $^{87}Sr/^{86}Sr$ throughout Phanerozoic time: Geology, v. 10, p. 516–519.

CANDER, H. S., KAUFMAN, J., DANIELS, L. D., AND MEYERS, W. J., 1988, Regional dolomitization of shelf carbonates in the Burlington-Keokuk Formation, Illinois and Missouri: Constraints from cathodoluminescent zonal stratigraphy, *in* Shukla, V. J., and Baker, P. A., eds., Sedimentology and Geochemistry of Dolostones: Soc. Econ. Paleontologists Mineralologists Spec. Publ. 43, in press.

CHAUDHURI, S., 1978, Strontium isotopic composition of several oilfield brines from Kansas and Colorado: Geochim. Cosmochim. Acta, v. 42, p. 329–331.

CHAUDHURI, S., BROEDEL, V., AND CLAUER, N., 1987, Strontium isotopic evolution of oilfield waters from carbonate reservoir rocks in Bindley Field, central Kansas, USA: Geochim. Cosmochim. Acta, v. 51, p. 45–53.

CHYI, M. S., HANSON, G. N., AND MEYERS, W. J., 1985, Isotope geochemistry of crinoids from the Burlington-Keokuk Fms.: Implications for diagenesis: Geol. Soc. America Abstr. w. Prog., v. 17, p. 547.

DEPAOLO, D. J., 1986, Detailed record of the Neogene Sr isotopic evolution of seawater from DSDP Site 590B: Geology, v. 14, p. 103–106.

DEPAOLO, D. J., AND INGRAM, B. L., 1985, High resolution stratigraphy with strontium isotopes: Science, v. 227, p. 938–941.

DEPAOLO, D. J., KYTE, F. T., MARSHALL, B. D., O'NEIL, J. R., AND SMIT, J., 1983, Rb-Sr, Sm-Nd, K-Ca, O, and H isotopic study of Cretaceous-Tertiary boundary sediments, Caravaca, Spain: Evidence for an oceanic impact site: Earth Planet. Sci. Letters, v. 64, p. 356–373.

GOLDSTEIN, S. J., AND JACOBSEN, S. B., 1987, The Nd and Sr isotopic systematics of riverwater dissolved material: Implications for the sources of Nd and Sr in seawater: Chem. Geol. (Isotope Geoscience Sect.), v. 66, p. 245–272.

GRANT, N. K., LASKOWSKI, T. E., AND FOLAND, K. A., 1984, Rb-Sr and K-Ar ages of Paleozoic glauconites from Ohio-Indiana and Missouri, USA: Isotope Geoscience, v. 2, p. 217–239.

HARLAND, W. B., COX, A. B., LLEWELLYN, P. G., PICKTON, C. A. G., SMITH, A. G., AND WALTERS, R., 1982, A geologic time scale: Cambridge, Cambridge Univ. Press, 131 p.

HARRIS, D. C., 1982, Carbonate cement stratigraphy and diagenesis of Burlington Limestones (Mississippian), southeastern Iowa and western Illinois [unpubl. master's thesis]: Stony Brook, State Univ. of New York, 297 p.

HESS, J., BENDER, M. L., AND SCHILLING, J. G., 1986, Evolution of the ratio of strontium-87 to strontium-86 in seawater from Cretaceous to present: Science, v. 231, p. 979–984.

KAUFMAN, J., HANSON, G. N., AND MEYERS, W. J., 1986, Constraints on the Sr isotopic composition of Mississippian (Osagean) seawater from analyses of nonluminescent brachiopods: Soc. Econ. Paleontologists Mineralogists Midyear Mtg., v. 3, p. 59.

KAUFMAN, J., CANDER, H. S., DANIELS, L. D., AND MEYERS, W. J., 1988, Calcite cement stratigraphy and cementation history of the Burlington-Keokuk Fm. (Mississippian), Illinois and Missouri: Jour. Sed. Petrology, v. 58, p. 100–116.

KOEPNICK, R. B., BURKE, W. H., DENISON, R. E., HETHERINGTON, E. A., NELSON, H. F., OTTO, J. B., AND WAITE, L. E., 1985a, Construction of the seawater $^{87}Sr/^{86}Sr$ curve for the Cenozoic and Cretaceous: Supporting data: Chem. Geol., v. 58, p. 55–81.

KOEPNICK, R. B., DENISON, R. E., AND HETHERINGTON, E. A., 1985b, Strontium isotope ratios from Arbuckle Group dolomites, Arbuckle Mountains, southern Oklahoma: Am. Assoc. Petroleum Geologists Research Conf. on Radiogenic Isotopes and Sedimentary Basins, Abstr., New Orleans, La.

KRALIK, M., 1984, Effects of cation-exchange treatment and acid leaching on the Rb-Sr system of illite from Fithian, Illinois: Geochim. Cosmochim. Acta, v. 48, p. 527–533.

LANE, H. P., AND DEKEYSER, T. L., 1980, Paleogeography of the late early Mississippian (Tournaisian 3) in the central and southwestern United States, *in* Fouch, T. D., and Magathan, E. R., eds., Paleozoic Paleogeography of West-Central United States, West-Central U.S. Paleogeography Symposium I, Rocky Mountain Section: Soc. Econ. Paleontologists Mineralogists, Denver, Colo., p. 149–162.

LINEBACK, J., 1968, Turbidites and other sandstone bodies in the Borden Siltstone (Mississippian) in Illinois: Illinois Geol. Surv. Circ. 425, 29 p.

LONG, L. E., AND AGEE, W. N., JR., 1985, Rb-Sr dating of a paleosol, Llano Uplift, Texas: Conference on Isotopes in the Sedimentary Cycle, Abstr., Obernai, France.

MCNUTT, R. H., FRAPE, S. K., AND FRITZ, P., 1984, Strontium isotopic composition of some Precambrian Shield brines: Isotope Geoscience, v. 2, p. 205–215.

MORTON, J. P., 1985, Rb-Sr dating of diagenesis and source age of clays in Upper Devonian black shales of Texas: Geol. Soc. America Bull., v. 96, p. 1043–1049.

MORTON, J. P., AND LONG, L. E., 1983, Rb-Sr dating of Paleozoic glauconite from the Llano region, central Texas: Geochim. Cosmochim. Acta, v. 44, p. 663–672.

ODIN, G. S., AND MATTER, A., 1981, De glauconiarum origine: Sedimentology, v. 28, p. 611–641.

PALMER, M. R., AND ELDERFIELD, H., 1985, Sr isotope composition of seawater over the past 75 Myr: Nature, v. 314, p. 526–528.

PETERMAN, Z. E., HEDGE, C. E., AND TOURTELOT, H. A., 1970, Isotopic composition of strontium in seawater throughout Phanerozoic time: Geochim. Cosmochim. Acta, v. 34, p. 105–120.

POPP, B. N., PODOSEK, F. A., BRANNON, J. C., ANDERSON, T. F., AND PIER, J., 1986, $^{87}Sr/^{86}Sr$ ratios in Permo-Carboniferous seawater from the analyses of well-preserved brachiopod shells: Geochim. Cosmochim. Acta, v. 50, p. 1321–1328.

PROSKY, J. L., AND MEYERS, W. J., 1985, Stoichiometry and trace element geochemistry of the Burlington-Keokuk dolomites: Soc. Econ. Paleontologists Mineralogists Midyear Mtg., v. 2, p. 73.

PROSKY, J. L., BANNER, J. L., AND MEYERS, W. J., 1986, Intrarhombic Fe and Mn trace element variations in early dolomites, Burlington-Keokuk Formation (Miss.) and their physiochemical implications: Soc. Econ. Paleontologists Mineralogists Midyear Mtg., v. 3, p. 91.

SALLER, A. H., 1984, Petrologic and geochemical constraints on the origin of subsurface dolomite, Enewetak Atoll: An example of dolomitization by normal seawater: Geology, v. 12, p. 217–220.

SIXT, S., 1984, Depositional environments, diagenesis, and stratigraphy of the Gilmore City Formation (Mississippian) near Humboldt, north-central Iowa [unpubl. mater's thesis]: Univ. of Iowa, Iowa City, 164 p.

STUEBER, A. M., PUSHKAR, P., AND HETHERINGTON, E. A., 1984, A strontium isotopic study of Smackover brines and associated solids, southern Arkansas: Geochim. Cosmochim. Acta, v. 48, p. 1637–1649.

SUNWALL, M., AND PUSHKAR, R., 1979, The isotopic composition of strontium in brines from petroleum fields of southeastern Ohio: Chem. Geol., v. 24, p. 189–197.

SWART, P. K., RUIZ, J. R., AND HOLMES, C. W., 1987, Use of strontium isotopes to constrain the timing and mode of dolomitization of upper Cenozoic sediments in a core from San Salvador, Bahamas: Geology, v. 15, p. 262–265.

THOMPSON, G. R., AND HOWER, J., 1973, An explanation for low radiometric ages from glauconite: Geochim. Cosmochim. Acta, v. 37, p. 1473–1491.

VEIZER, J., 1983, Chemical diagenesis of carbonates: Theory and application of the trace element technique, *in* Stable Isotopes in Sedimentary Geology: Dallas, Tex., Soc. Econ. Paleontologists Mineralogists Short Course No. 10, p. 3-1–3-100.

VEIZER, J., COMPSTON, W., CLAUER, N., AND SCHIDLOWSKI, M., 1983, $^{87}Sr/^{86}Sr$ in Late Proterozoic carbonates: Evidence for a "mantle" event at approx. 900 Ma ago: Geochim. Cosmochim. Acta, v. 47, p. 295–302.

WADLEIGH, M. A., VEIZER, J., AND BROOKS, C., 1985, Strontium and its isotopes in Canadian rivers: Fluxes and global implications: Geochim. Cosmochim. Acta, v. 49, p. 1727–1736.